An Automatic Random Walk Based Method for 3D Segmentation of the Heart in Cardiac Computed Tomography Images

Conference Paper · April 2018

DOI: 10.1109/ISBI.2018.8363822

CITATIONS
0

READS
72

4 authors, including:

Vy Bui
The Catholic University of America
11 PUBLICATIONS **46** CITATIONS

SEE PROFILE

Lin-Ching Chang
The Catholic University of America
54 PUBLICATIONS **1,322** CITATIONS

SEE PROFILE

2018 IEEE 15th International Symposium on Biomedical Imaging (ISBI 2018)
April 4-7, 2018, Washington, D.C., USA

An Automatic Random Walk Based Method for 3D Segmentation of The Heart In Cardiac Computed Tomography Images

Vy Bui[1,2], Li-Yueh Hsu[1], Lin-Ching Chang[2], Marcus Y. Chen[1]

[1]National Heart, Lung and Blood Institute, National Institutes of Health, Bethesda, Maryland, USA
[2]Department of Electrical Engineering and Computer Science, The Catholic University of America, Washington, DC, USA
01bui@cua.edu, lyhsu@nih.gov, changl@cua.edu, chenmy@nih.gov

ABSTRACT

Cardiac Computed Tomography (CT) is an important imaging modality for diagnosing cardiovascular disease. Heart segmentation from CT scans is a prerequisite for clinical interpretation, providing critical information for quantitative analysis of the heart and coronary structures. This paper presents a fully automated algorithm for heart segmentation based on the random walk model and automated initial seeds detection. The performance of the method is evaluated on a cardiac CT dataset of 58 subjects using manual segmentation as a reference standard. We show the results of our method are similar to the reference standard and are comparable to the results from a commercial product. We also demonstrate our automated method can reliably segment other tissue structures in cardiac CT images.

Index Terms— Heart Segmentation, Cardiac CT, Random Walk

1. INTRODUCTION

Cardiac Computed Tomography (CT) is a main imaging modality for assessing the morphology of the heart and coronary arteries for diagnosing cardiovascular disease. Accurate and automated heart segmentation in cardiac CT images is an important task for evaluating cardiac and coronary artery structures. It is also the first step for quantitative assessment of aorta, coronary arteries, myocardium, and different cardiac chambers. However, automated segmentation in cardiac CT image can be challenging due to similar signal intensity of the heart with its surrounding organs as well as a large variation of the heart shape.

Several previous works have presented different approaches to segment both the chambers and great vessels as a whole [1-6], the chambers as well as descending aorta [7], or focus on separating the heart chambers [8-12]. Some of the prior works that are atlas-based or registration-based [1, 2] may not be suitable for routine clinical applications due to high computational cost, e.g., 20-30 minutes per CT volume.

We aim to develop a fast and fully automatic method to segment the heart as well as separate different tissue structures in the cardiac CT images, e.g., lung, chest wall, spine, descending aorta, and liver. The proposed method is based on the random walk algorithm [13] that segments a region of interest from a set of initial seed points. We incorporate multiple image processing stages with domain knowledge to extract seed points from different tissue structures automatically. These seeds are then used for the 3D random walk algorithm to perform final segmentation.

2. METHODS

The random walk algorithm solves a diffusion equation with tracers initiated at the position of different seeds [13]. The local diffusivity coefficient will be greater if neighboring voxels share similar intensities. However, it will be hard for diffusion to cross high gradient regions if voxels have large intensity variations. During such diffusion process, the label of each unknown voxel is attributed to the seed label that has the highest probability. The seeds selected in random walk algorithm play a vital role in obtaining a robust and efficient segmentation [14, 15]. Therefore, it is important to obtain initial seed points inside the region of interest and label other surrounding tissue structures as background. Unlike the original work that requires the user to interactively provide a set of pre-defined labels or seeds, we aim to develop a new method that can select the initial seeds automatically for the random walk segmentation with the application to cardiac CT images.

2.1. Data Description and Preprocessing

The method was tested on contrast-enhanced CT angiography study of 58 patients. All studies were performed under procedures and protocols approved by our institutional review board. Each study contains between 240

and 520 images with a slice thickness of 0.5 mm and a spacing of 0.25 mm or 0.5 mm. Each image has 512×512 pixels with a pixel size ranged from 0.29×0.29 mm^2 to 0.43×0.43 mm^2. To improve the symmetrical property of the voxel for 3D image processing, all images were subsampled to an isotropic voxel size of 1.0×1.0×1.0 mm^3 for processing.

As the Hounsfield units (HU) are used in CT images to display attenuation coefficient of different tissues, pixel intensity values in the images were converted to HU from a range of -1024 to +3071 to display different substances from air to bone and metallic objects. Each tissue in the images can be characterized by a limited range of HU. However, tissues in different organs can share similar HU which makes simple thresholding techniques not practical.

2.2. Seed Masks Segmentation

As shown in Figure 1, our method includes several sequential image processing stages to automatically extract different tissue masks from a cardiac CT angiography volume. These segmentation steps generate different labels of seed masks for the final random walk segmentation.

2.2.1. Lung, chest wall and spine mask

Several non-cardiac structures are detected by thresholding and mathematical morphology processing in stage 1. First, the lung mask is characterized by intensities between -1000 and -400 HU. Next, bone structures are detected using a threshold value greater than 300 HU. The rib mask is located above the lung, while the spine mask is separated at the lower part of the images. After obtaining the rib, the chest wall mask is detected using a threshold value above 0 HU, followed by 3D morphological erosion with a sphere and followed a cylinder structure element to separate possible inclusion of the heart tissues.

2.2.2. High contrast enhancement masks

High contrast enhancement masks are estimated in stage 2 which include aorta, left atrium, and left ventricle. First, an ellipse area is fitted to the lung and the chest wall structures. 3D morphological skeletonization was performed on the lung and the chest wall before the polynomial fitting. This step effectively removes high intensity voxels in the surrounding non-heart regions. From the ellipse volume, adaptive thresholding is then performed to select high intensity voxels for random walk segmentation to segment ascending aorta, left chambers (AA-LC) mask. Next, the descending aorta is segmented by the same adaptive threshold value from the prior step but excluding the AA-LC mask. It is then followed by morphological processing to isolate the largest 3D structure as the final descending aorta mask.

2.2.3. Intermediate contrast enhancement masks

Right atrium, right ventricle and myocardium are determined in stage 3. An adaptive thresholding is performed by selecting an initial lower threshold as the peak of the intensity histogram within 0 to 100 HU range. This threshold is then gradually decreased by the estimated size of right chambers (RC) until it reaches to 60% of the AA-LC size. The upper threshold is set based on the median value of AA-LC mask. Next, the myocardium is estimated with an intensity range between 40 and 150 HU and a distance within 5 mm to AA-LC and RC. An ellipse area obtained in 2.2.2 is used to exclude similar intensity voxels in the chest wall and liver.

2.2.4. Heart mask

The ascending aorta, left, right chambers, and myocardium are combined as a single mask in stage 4 to assemble the heart mask. A good estimate of the heart mask is attained at this stage except possible exclusion of the great vessels from previous morphological processing. Therefore, the heart mask is expanded to include the voxels that have

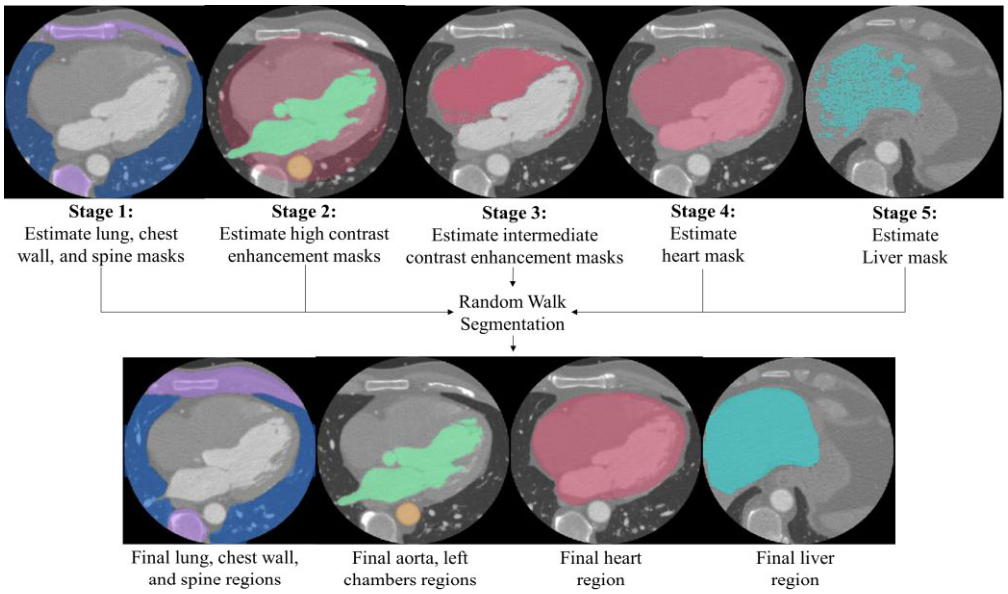

Figure 1. Workflow of the proposed multi-label segmentation algorithm for cardiac CT images

intensity above 200 HU and a distance within 3 mm to the chambers. A 3D closing morphological processing is then applied to obtain the final mask of the heart.

2.2.5. Liver mask

The liver mask is estimated in stage 5 using a threshold value between 0 and 200 HU and subtracting the other tissues detected from the previous stages within the volume. It is followed by morphological processing to separate the largest 3D structure as the final liver mask.

2.3. Random Walk Segmentation

The random walk segmentation algorithm requires pre-defined seeds inside the region of interest, either manually or automatically [13-15]. In our method, such seed masks are automatically determined by the previous 5 initial segmentation stages. These initial masks are then used for random walk algorithm to refine the final multi-tissue structure segmentations, i.e., heart, lung, chest wall, descending aorta, spine, and liver. Random walk segmentation is first applied by using the heart mask as foreground seeds and other masks i.e., lung, chest wall, liver, labeled as background seeds. Likewise, random walk is run repeatedly with a different set of foreground seeds to refine the lung, chest wall, and liver segmentations; except the descending aorta since it was already well separated during the initial segmentation.

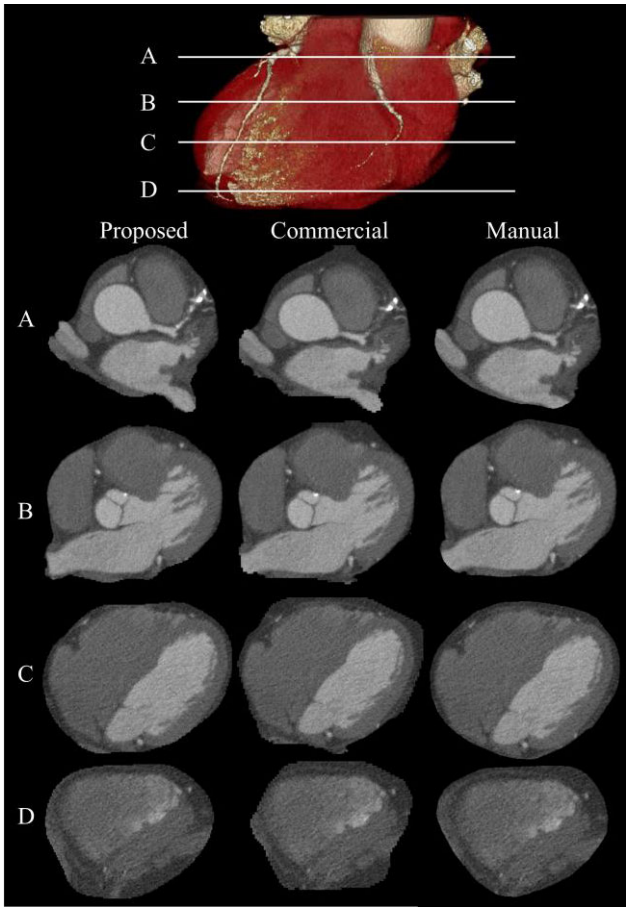

Figure 2. Qualitative comparison of heart segmentation result.

2.4. Performance Comparisons

The results of our method were assessed using a reference standard defined by manual segmentation from 58 cardiac CT studies. The manual segmentation of the heart was supervised by an expert cardiologist using a dedicated commercial workstation (Vitrea Core Client 6.7.0, Vital Images). Additional comparison was also made between our automated heart segmentation and the results from the Vitrea workstation. Segmentation quality was evaluated using Dice coefficient, Hausdorff distance (HD) and mean surface distance (MSD).

3. RESULTS AND DISCUSSION

Figure 2 shows a qualitative comparison of automatic vs. manual heart segmentation. Quantitative comparisons of the proposed and the commercial segmentations are summarized in Table 1. There is no significant difference in Dice and MSD between the two methods using a paired test (p=NS). However, our results have a smaller Hausdorff distance than the commercial segmentation ($p<0.05$). Therefore, our method is reliable and provides comparable or better results compared to the commercial software for heart segmentation.

The computational time of our method is 1.88±0.71 minutes for the heart segmentation and 2.52±0.87 minutes for segmenting all tissue structures including lung, chest wall, liver, descending aorta and spine. The method was implemented in Python with Scikit image processing library [16]. All studies were processed with the same parameter settings under a desktop computer with an Intel Core i7-6950X 3.00GHz CPU and 64GB RAM.

Previous works that developed automated heart segmentation in cardiac CT images have presented their results using similar quality metrics with manual segmentation. An atlas-based method has reported an MSD of 0.99 mm based on a small dataset of 8 patients [1]. An MSD ranged from 0.83 to 1.39 mm was also reported based on 20 CT cases scanned from multi vendors [1]. A graph cut based method has reported a MSD of 5.5 mm based on 70 cases [3]. A Haar classifier and active shape model based method has presented a maximum closest distance of 3 to 5 mm based on 5 cases [6]. A similar work to our approach has been presented and tested on 32 cases [7]. However,

	Proposed vs. Commercial	Proposed vs. Manual	Commercial vs. Manual	p-value
Dice	0.92 ± 0.04	0.92 ± 0.02	0.92 ± 0.04	NS
MSD (mm)	2.79 ± 1.64	2.71 ± 0.63	2.70 ± 1.46	NS
HD (mm)	19.43 ± 13.31	18.20 ± 5.32	22.75 ± 13.28	<0.05

Table 1. Comparison of automatic heart segmentation with the reference standard. Results are expressed as mean ± standard deviation. (HD: Hausdorff distance. MSD: mean surface distance. NS: non-significant, p>0.05)

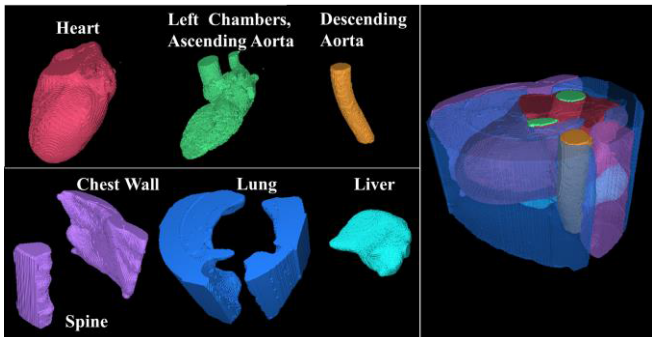

Figure 3. 3D multi-color render of different tissue structures in a cardiac CT volume segmented by the proposed algorithm.

their method includes the descending aorta, but excludes great vessels from the heart region. In terms of computational time, our method is faster than [1,2] and comparable to [7] but slower than [3,6]. Another segmentation approach based on machine learning has also reported successful results [4,5]. It has the fastest computation speed once the model is trained, but the training time was not mentioned.

In addition to the heart segmentation, our proposed method can also segment different tissue structures in the cardiac CT images (see Figure 3). The ranges of the HU for different tissue structures segmented by our automated method are shown in Figure 4.

This multi-tissue segmentation feature is useful for image context-driven annotation of cardiac CT dataset, such as a similar work performed on abdomen CT for multi-label image annotation [17]. However, future work is needed to assess the segmentation results of these non-cardiac tissues and to classify coronary artery structures, myocardium and different cardiac chambers within the heart region.

4. CONCLUSIONS

An automatic 3D random walk based segmentation method for cardiac CT images is presented in this paper. It combines domain knowledge and pipeline image processing techniques to detect initial regions of interest for different tissues in the CT volume. A 3D random walk approach is then used for the final segmentation. We show the method worked well in different clinical cardiac CT datasets. We also show the results of our heart segmentation are similar to the manual segmentation, and are comparable to the results from a commercial product. The proposed method can be used to assist the segmentation of coronary structure and different heart chambers in our future work.

5. REFERENCES

[1] Kirişli HA, et al., “Evaluation of a multi-atlas based method for segmentation of cardiac CTA data: a large-scale, multicenter, and multivendor study.” Medical physics, 37, 6279, 2010.

[2] Van Rikxoort EM, et al., “Adaptive local multi-atlas segmentation: Application to heart segmentation in chest CT scans.” SPIE Medical Imaging, 6914, 2008.

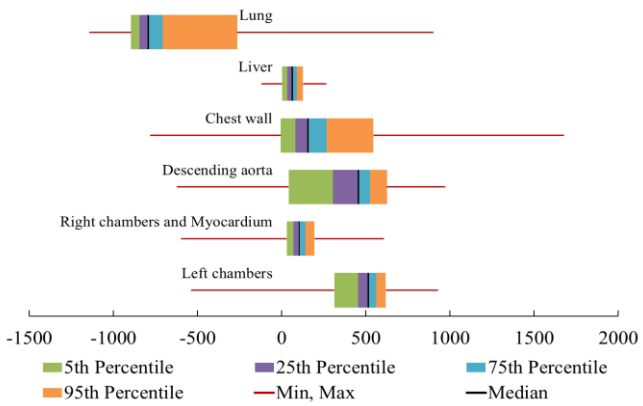

Figure 4. The ranges of the HU measured from automated segmented tissue structures in 58 cardiac CT dataset.

[3] Funka-Lea G, et al., “Automatic heart isolation for CT coronary visualization using graph-cuts.” IEEE Biomedical Imaging: Nano to Macro, 614, 2006.

[4] Zheng Y, et al., “Fast and automatic heart isolation in 3D CT volumes: Optimal shape initialization.” MICCAI, 84, 2010.

[5] Zhong H, et al., “Automatic heart isolation in 3D CT images.” MICCAI, 165, 2012.

[6] Ma F., et al., "Automatic Segmentation of the Full Heart in Cardiac Computed Tomography Images Using a Haar Classifier and a Statistical Model." Journal of Medical Imaging and Health Informatics, 6, 1298-1302, 2016.

[7] Larrey-Ruiz J, et al., “Automatic image-based segmentation of the heart from CT scans.” Journal on Image and Video Processing, 1, 52, 2014.

[8] Mortazi A, et al., “Multi-planar deep segmentation networks for cardiac substructures from MRI and CT.” arXiv, 1708.00983, 2017.

[9] Shahzad R, et al., “Automatic segmentation and quantification of the cardiac structures from non-contrast-enhanced cardiac CT scans.” Physics in Medicine and Biology, 62, 3798, 2017.

[10] Ecabert O, et al., “Automatic model-based segmentation of the heart in CT images.” IEEE transactions on medical imaging, 27, 1189, 2008.

[11] Zheng Y, et al., “Four-chamber heart modeling and automatic segmentation for 3D cardiac CT volumes using marginal space learning and steerable features.” IEEE transactions on medical imaging, 27, 1668, 2008.

[12] Cai K, et al., “A framework combining window width-level adjustment and Gaussian filter-based multi-resolution for automatic whole heart segmentation.” Neurocomputing, 220, 138, 2017.

[13] Grady L, “Random walks for image segmentation.” IEEE transactions on pattern analysis and machine intelligence, 28, 1768, 2006.

[14] Grady L, et al., “Random walks for interactive organ segmentation in two and three dimensions: Implementation and validation.” MICCAI, 773, 2005.

[15] Zheng Y, et al., “Feature learning based random walk for liver segmentation.” PloS one, 11(11), 2016.

[16] Van der Walt S., et al., "scikit-image: image processing in Python." PeerJ 2, 2014

[17] Xue Z, et al., “Automatic multi-label annotation of abdominal CT images using CBIR.” SPIE Medical Imaging, 1013807, 2017.